

# An analysis of seasonal predictability in coupled model forecasts

P. Peng · A. Kumar · W. Wang

Received: 22 June 2009 / Accepted: 20 November 2009 / Published online: 3 December 2009  
© US Government 2009

**Abstract** In the recent decade, operational seasonal prediction systems based on initialized coupled models have been developed. An analysis of how the predictability of seasonal means in the initialized coupled predictions evolves with lead-time is presented. Because of the short lead-time, such an analysis for the temporal behavior of seasonal predictability involves a mix of both the predictability of the first and the second kind. The analysis focuses on the lead-time dependence of ensemble mean variance, and the forecast spread. Further, the analysis is for a fixed target season of December–January–February, and is for sea surface temperature, rainfall, and 200-mb height. The analysis is based on a large set of hindcasts from an initialized coupled seasonal prediction system. Various aspects of predictability of the first and the second kind are highlighted for variables with long (for example, SST), and fast (for example, atmospheric) adjustment time scale. An additional focus of the analysis is how the predictability in the initialized coupled seasonal predictions compares with estimates based on the AMIP simulations. The results indicate that differences in the set up of AMIP simulations and coupled predictions, for example, representation of air–sea interactions, and evolution of forecast spread from initial conditions do not change fundamental conclusion about the seasonal predictability. A discussion of the analysis presented herein, and its implications for the use of AMIP simulations for

climate attribution, and for time-slice experiments to provide regional information, is also included.

## 1 Introduction

Predictability of different component of the Earth System can be described following two paradigms (Lorenz 1969). The predictability of first kind refers to information contained in the initial conditions, and its quantification entails analyzing separation of forecast trajectories from slightly perturbed initial conditions. Further, predictability is retained to a lead-time up to which the time-evolving phase space of an ensemble of forecasts can be distinguished from the reference climatological distribution.

In an alternate scenario, even though the system may have moved away from the influence of the initial conditions, in response to the slowly varying external forcing, distribution of possible outcomes that are consistent with the external forcing may differ from the reference climatological distribution. This difference provides the basis for the predictability of the second kind. For example, the dependence on the slowly varying sea surface temperature (SST) of the atmospheric state belongs to the second kind of predictability.

At many operational centers, dynamical seasonal forecasts using coupled models are now routinely made. Such prediction systems involve initialization of different components of the coupled system, for example, ocean and atmosphere, and a forward integration of a large ensemble of predictions from slightly different initial states. The analysis of the lead-time dependence of predictability of different variables in long-range initialized predictions involves flavors of predictability of both the first and the second kind, and is the focus of this paper.

---

P. Peng · A. Kumar · W. Wang  
Climate Prediction Center, NOAA,  
Washington, DC, USA

A. Kumar (✉)  
Climate Prediction Center, NCEP/NWS/NOAA,  
5200 Auth Road, Rm 800, Camp Springs,  
MD 20746, USA  
e-mail: arun.kumar@noaa.gov

For seasonal climate forecasts, the analysis of predictability of slowly varying variables, for example, SST falls under the paradigm of the predictability of the first kind. Up to what time-scale SSTs, particularly in the tropical eastern Pacific related to the El Niño-Southern Oscillation (ENSO) variability, are predictable remains an open question. Assessment of SST predictability is also complicated by a lack of consensus on the relative role of ocean dynamics and stochastic forcing (for example, related to the westerly wind bursts), and ENSO predictability estimates extending up to more than a year have been reported (Chen et al. 2004; Luo et al. 2008). An added complicating factor in estimating the predictability of ENSO SST is its decadal modulation (Tang et al. 2008). Away from the core region of ENSO SST variability, time-scale of SST predictability in other ocean basins is estimated to be much lower.

The lead-time dependence for the forecast of atmospheric variables, on the other hand, follows a mix of predictability of the first and the second kind. For predictions from a short lead-time, predictability of the first kind is important. Experience with the weather forecasts, and from the basic understanding of growth of perturbations with time, it is estimated that the influence of initial conditions on daily atmospheric fields does not extend beyond 2 weeks. By time averaging (for example, weekly or monthly averages), at the expense of temporal resolution and specificity of information, the influence of initial condition can be extended a bit further (Weigel et al. 2008; Chen et al. 2009). However, for forecasts with longer leads, predictable information falls under the paradigm of the predictability of the second kind and the source of predictable information is due to the slowly varying boundary conditions, SST in particular.

For the atmospheric seasonal variability, the predictability of second kind due to the interannual variability in SST has been extensively studied based on the so called Atmospheric Model Intercomparison Project (AMIP) simulations (Kumar and Hoerling 1995; Harzallah and Sadourny 1995; Rowell 1998; Trenberth et al. 1998; Zwiers et al. 2000; Kusunoki et al. 2001; Kumar et al. 2003). At times, however, estimates of predictability based on the AMIP simulations, have been questioned since AMIP simulation do not include coupled air-sea interaction (van den Dool et al. 2006). There is also a possibility that for shorter lead-time seasonal predictions, information from the initial conditions may also influence of estimates of predictability and alter estimates based on the AMIP simulations.

With this background, the purpose of the analysis is to quantify the lead-time dependence of predictability based on a large set of hindcast from a coupled seasonal climate forecast system. The analysis includes how the signal-

to-noise (and predictability) for slow (e.g., SST) and fast (e.g., atmospheric) variables evolve with the lead-time. For the atmospheric variables, the analysis also provides an opportunity to compare the predictability estimates based on a coupled initialized system to that obtained from the AMIP simulations. This comparison is of importance as the AMIP simulations are one of the key tools for attribution analysis of climate anomalies due to different forcings (Barnston et al. 2005; Hoerling et al. 2008a, b), and are also used in time-slice experiments to provide information on a much higher resolution under various climate projection scenarios.

The analysis complements recent efforts analyzing the prediction skill in initialized coupled forecast system (Palmer et al. 2004; Luo et al. 2005; Kug et al. 2008; Wang et al. 2008; Jin et al. 2008), and extends the scope further to understand the lead-time dependence of predictability and prediction skill for SSTs and atmospheric variables. The coupled forecast system, the hindcasts, and the observational data is described in section 2. Results are presented in section 3, and a summary, with further discussions appears in Sect. 4.

## 2 Data and analysis procedures

The analysis is for a fixed target season of December–January–February (DJF), and includes initialized coupled predictions from different lead-times. DJF was selected for the reason that the interannual variance of equatorial Pacific SST anomalies is largest for this season, and tropical-extratropical teleconnections have the strongest amplitude (Newman and Sardeshmukh 1998; Kumar et al. 2003; Trenberth et al. 1998). Further, boreal winter is also the season for which extensive literature documenting predictability of seasonal means based on the AMIP simulations exists (Trenberth et al. 1998; Hoerling and Kumar 2002). The analysis is for the predictions of SST (the forcing for the atmosphere), rainfall (the variable through which the influence of anomalous SST is communicated to the atmosphere), and 200-mb height (a variable for which the global teleconnections are most well defined).

The analysis is based on the archive of extensive hindcasts from NCEP Coupled Forecast System (CFS). The characteristics and model description of the CFS is documented by Wang et al. (2005) and Saha et al. (2006).

The CFS hindcasts are clustered in five initial conditions around the 1st, 11th, and 21st of the month and span the 1981–2006 period. For DJF—the target predicted season—forecast with 0-month lead, 1-month lead, etc. are defined in the following manner: DJF predictions with 0-month lead include all 15 initial conditions from November; 1-month lead DJF predictions include initial conditions from October; 6-month lead predictions include initial

conditions from May. Since CFS forecasts extend to 9-months, 6-months is the longest lead seasonal forecast that can be analyzed.

For each lead-time, the ensemble mean prediction is defined as the average of 15 individual members, and ensemble mean variance (EMV) is defined as the variance of ensemble means over the 26-year analysis period. The forecast spread is defined as the variance of departure in the individual members from the ensemble mean. The relative magnitude of the EMV to the amplitude of forecast spread is the signal-to-noise (SN) ratio, and is a measure of the level of seasonal predictability. For the atmospheric variables, following the traditional analysis of variance technique (Kumar and Hoerling 1995; Rowell 1998), EMV is equivalent to the external variability (this terminology follows the AMIP simulations), and the forecast spread is the internal variance.

Predictability estimates from the CFS seasonal forecasts are also compared with those obtained from the AMIP simulations using the atmospheric component of the CFS. An 18-member ensemble of such simulations is available from the 1996–2009 period, and although the comparison is not ideal (in that the analyses period differ), it does allow us to compare the large-scale spatial features of different components of seasonal variability.

The observed seasonal mean for the SST, rainfall, and 200-mb heights are from the optimal interpolation (OI) SST (Reynolds et al. 2002), CMAP precipitation (Xie and Arkin 1997) and the DOE/NCEP Reanalysis-2 (Kanamitsu et al. 2002), respectively. Finally, the anomaly for the observations and predictions are obtained from their own climatologies defined over the 1981–2006 period, and for the 1996–2007 for the AMIP simulations.

### 3 Results

We begin our discussion with the assessment of forecast bias for selected fields with lead-time. This analysis also helps interpret some of the results discussed subsequently. The bias for the respective field is defined as the difference between observed and model predicted DJFs averaged over the analysis period. Shown in Fig. 1 are the biases for the SST and 200-mb height for 0-month and 6-month lead forecasts. As the forecast lead-time increases, the SST bias (Fig. 1, top right), in general, also increases (an exception is the extratropical latitudes in the southern hemisphere). The RMS bias averaged over the tropical latitudes between 20°S and 20°N increases from 0.47 to 0.82, while the RMS bias average over the globe changes from 1.64 to 1.49. The major features for the SST bias include: colder SSTs in tropical regions; warmer SSTs to the western part of continents that coincide with the regions of persistent stratus

decks; and general warming in the southern latitude extratropics. The last two features are related to underestimation of stratus and low-level clouds by the CFS leading to an overestimation of shortwave flux into the oceans. Apart from a general increase in the amplitude of the SST bias, the spatial structure of the bias itself is fairly similar for the two lead-times.

The 200-mb height forecast bias (Fig. 1, middle row) has below normal heights almost over the entire globe. The bias becomes larger for the longer lead-time, a feature consistent with the tendency for larger colder SST bias for longer lead-time predictions. The zonally asymmetric bias for the 200-mb height (Fig. 1, bottom panels) illustrates remarkable similarity in the spatial structure for the shortest and the longest lead-time forecasts, with spatial anomaly correlation of 0.91. The spatial similarity of bias for different lead-times is in agreement with the long-standing view that model biases in general circulation models set up early during the integration, and is consistent with earlier results (Phelps et al. 2004).

We next compare the lead-time dependence of the standard deviation of seasonal means, and its decomposition into the EMV and the forecast spread (also referred to as the internal variance). We start with the comparison of standard deviation between observed and model predicted seasonal means to (a) assess the realism of model predicted seasonal variability, and (b) assess how does it evolves with the lead-time. *We should point out that our analysis is for a fixed target season, and focuses on the assessment of changes in variability of ensemble of forecasts with different lead-time. The analysis is not for how various components of variability evolve starting from an ensemble of initial conditions.*

The variability of seasonal SST, rainfall, and 200-mb height for observations and model prediction with the shortest lead is shown in Fig. 2. The amplitude and the spatial structure for all three variables compares reasonably well. For example, observed SSTs have largest variability in the equatorial tropical Pacific between the dateline and 120°W related to ENSO. This feature is also well replicated in model predictions with 0-month lead, and by and large, reflects the basic persistence of initial SST anomalies. For the variability of DJF rainfall, the largest amplitude of which is in the tropical latitudes, model variability has larger amplitude than the observations. As is generally the case for the rainfall comparison, it is not easy to discern if this is due to deficiencies in the observed estimates of the oceanic rainfall or is a feature of model bias. Finally, the spatial structure of seasonal variability of 200-mb heights for the model and observations compares well.

In Fig. 2 (right panel) the evolution of seasonal mean variability for 6-month lead forecast is assessed as the ratio of variability for the 0-month forecast. A ratio of

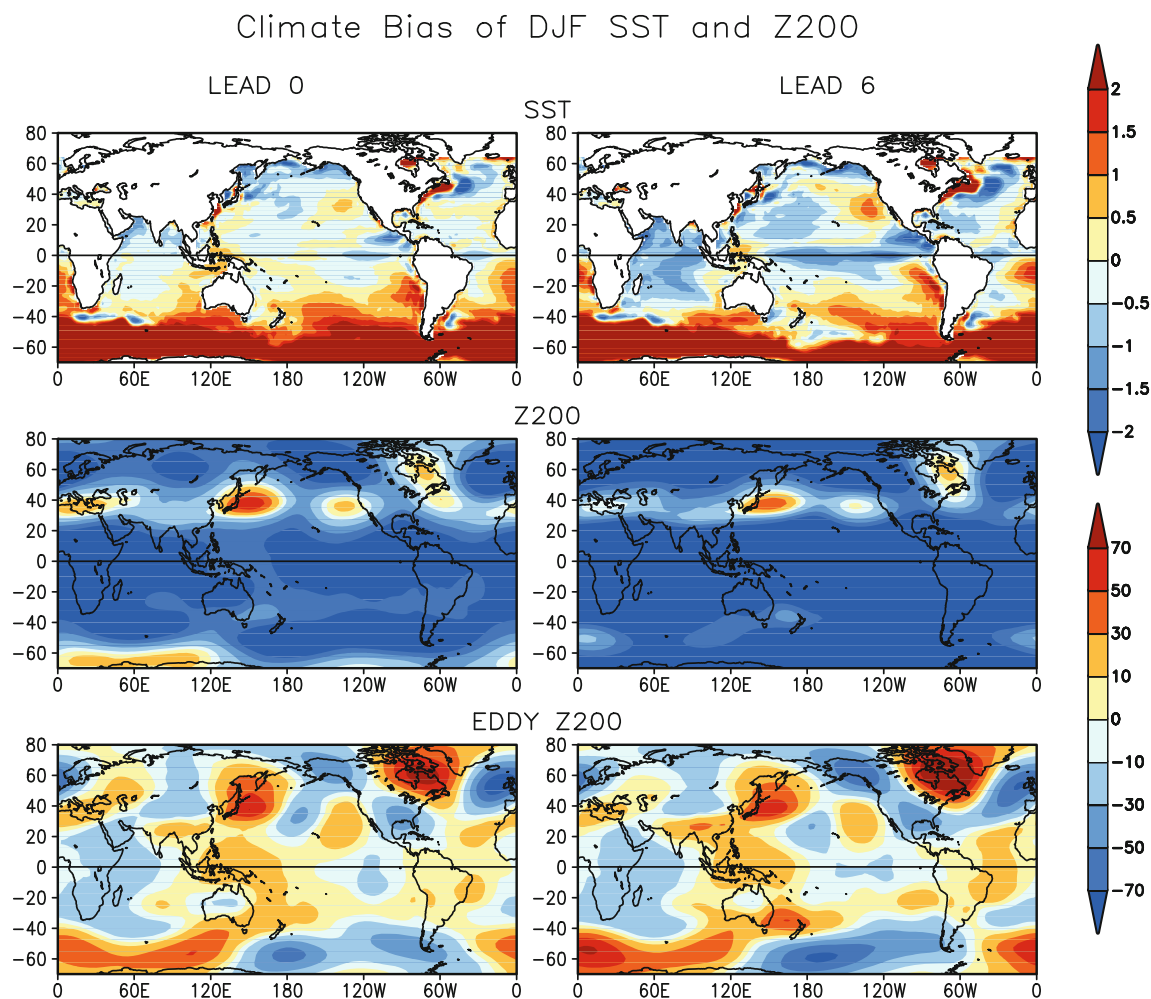


**Fig. 1** DJF seasonal mean bias for 0-month lead (left column) and 5-month lead forecasts for SST (top row, units °K), 200-mb heights (middle row, units meters), and 200-mb eddy heights (bottom row,

units meters). Bias is computed as the difference between the observed and forecast climatology over the 1981–2006 period

greater (less) than one implies that standard deviation of DJF anomalies for the 6-month lead prediction is larger (smaller) than the standard deviation for the corresponding 0-month lead prediction. Although this comparison does not provide a unanimous direction for the change in standard deviation at all locations, for rainfall and 200-mb heights, regions with smaller standard deviation for 6-month lead-time dominate. This is quantified by the fraction of cosine-weighted area of 63% (for rainfall), and 65% (for 200-mb heights) for which standard deviation for 6-month lead prediction is smaller. This fraction is 66% for the SSTs.

There are multiple factors that could affect the lead-time dependence of the seasonal variability making it harder to anticipate how this quantity should behave. For example, one would expect that the EMV would decrease with lead-time as the skill of ensemble mean prediction, consistent with the notion of predictability of first kind, also decreases

with lead-time. In other words, *for the fixed target season*, the ensemble means evolve toward the climatology. At the same time, one would also expect forecast spread among different ensemble members to increase. The competing influences, and their lead-time dependence (which could be parameter and location dependent), could result in a complicated behavior for the evolution of total variability itself. Another complicating factor is that for certain variables, e.g., rainfall, variability depends critically on the mean state of another variable, e.g., SST, and lead-time dependence of bias for the latter may have a large influence on the former.

The analysis of the lead-time dependence in the evolution of EMV and internal variance is next discussed. The results for the EMV for 6-month, 0-month lead predictions and their ratio are shown in Fig. 3. To understand the evolution of the EMV, it is helpful to start with SST, as the EMV for the atmospheric variables, due to fast adjustment

STDV of SST, PRATE and Z200 (DJF 82–07)

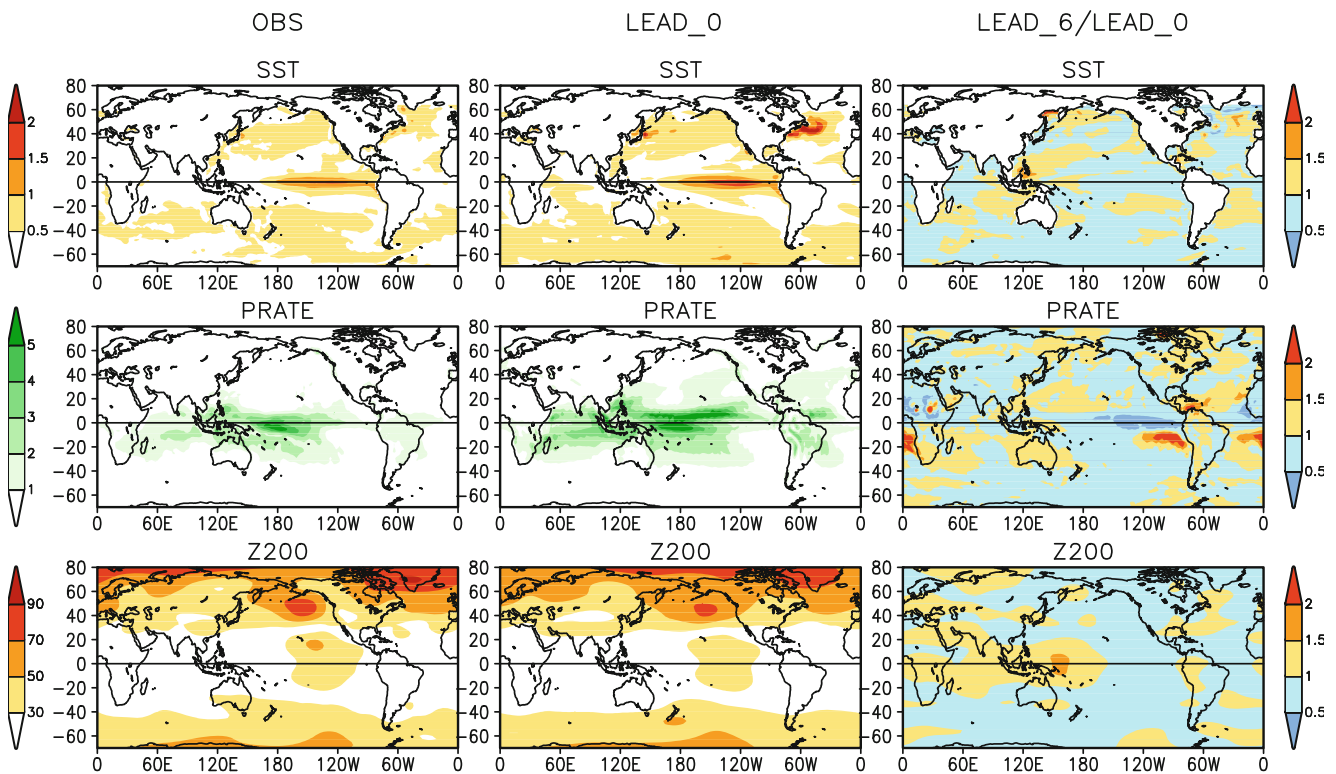


**Fig. 2** Standard deviation of DJF seasonal mean for SST (top row, unit °K), rainfall (middle row, units mm/day), and 200-mb heights (bottom row, units meters). The left panels are the standard deviation for the observations, while the middle panels are the standard deviations for the 0-month lead forecasts. The standard deviation for

the 6-month lead forecasts is shown as the ratio of standard deviation relative to the standard deviation for the 0-month forecasts. Further, ratio of greater (less) than one indicate when the standard deviation for the 6-month forecast is larger (smaller) than the standard deviation for the 0-month lead forecast

time-scale, is likely influenced by SSTs (i.e., is basically determined by the predictability of the second kind).

For the SST predictions, it is helpful to consider the following conceptual picture: An ensemble of coupled model predictions starts from a cluster of slightly different SST initial conditions. As the model predictions approach the target season, individual predictions would have larger spread. Therefore, for a fixed target season, one would expect that the spread of seasonal means (among various ensemble members) would be small for shorter lead-time predictions and becomes larger as the lead-time increases. As a consequence, we anticipate that the ratio of internal variance for prediction from 6-month lead to that for prediction with 0-month lead would be greater than one. For the lead-time dependence of EMV (and for forecasts for a fix target season), the reverse is expected to happen, i.e., the ensemble mean SST state is likely to evolve towards the climatological mean leading to smaller standard deviation for ensemble means. In the limit of very long lead-time predictions, one would expect EMV to asymptote to zero.

Lead-time dependence of the EMV for the SST in Fig. 3 (top row) fits the conceptual picture very well. Except for a few locations, the ensemble mean variance of SST for the 6-month lead prediction is indeed smaller than for the 0-month lead prediction. Exceptions include larger variance near the maritime continent and in the extratropical Atlantic southeast of Greenland. The reason for this behavior is not immediately clear. One possibility is that it might be related to emergence of pre-existing sub-surface ocean temperature anomalies in the majority of predictions.

For rainfall, the EMV for 6-month lead prediction is smaller than for the 0-month lead prediction (Fig. 3, middle row). There are few geographical regions, however, where EMV for longer lead forecasts is much higher (e.g., regions to the west of the continents), and further, these areas do not coincide with the regions of increase in EMV for SST (Fig. 3, top row). These regions, on the other hand, do coincide with regions with substantial warm SST biases for longer lead (Fig. 1, left column). Warmer mean SST states are more conducive to rainfall (Gadgil et al. 1984) resulting in an increase in rainfall variability.

## STDV OF ENSEMBLE MEAN (DJF 82–07)

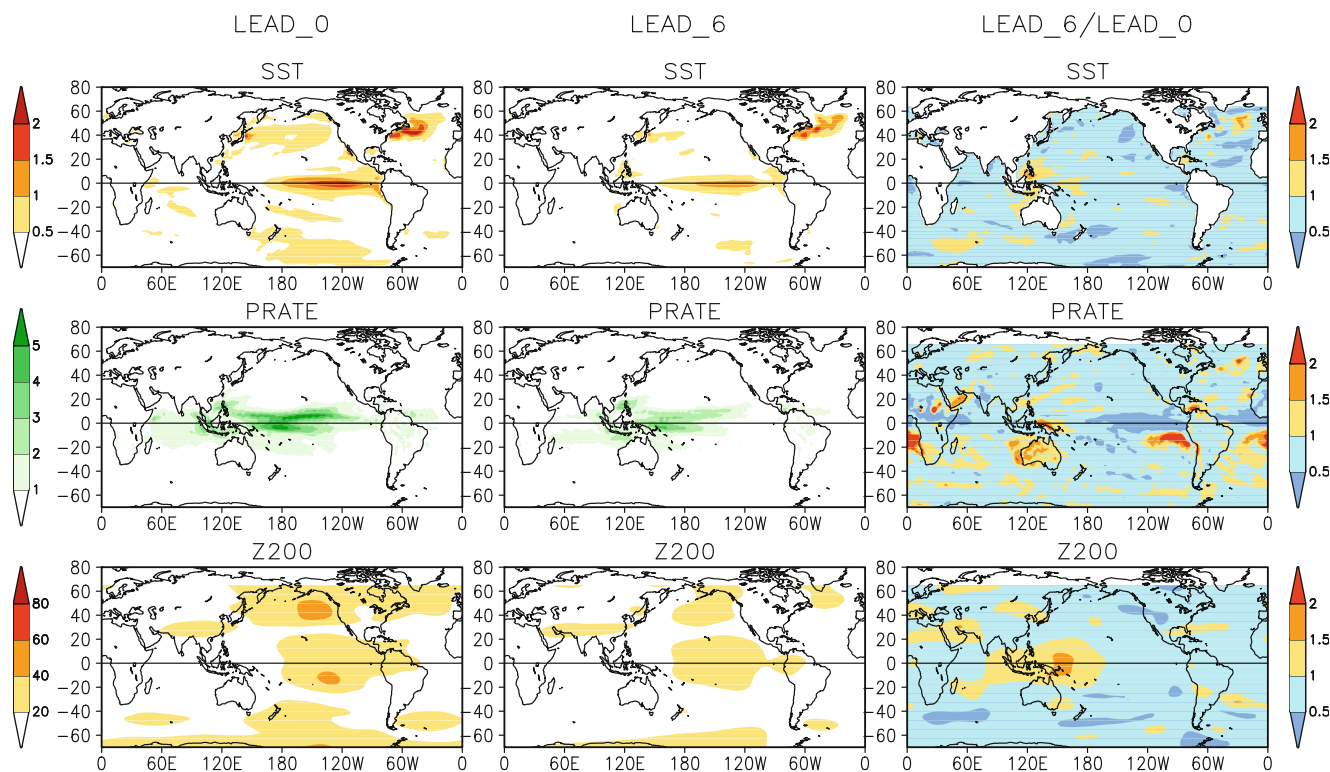


**Fig. 3** Standard deviation of ensemble averaged DJF seasonal means for 0-month lead forecasts (*left column*), 6-month lead forecasts (*middle column*), and ratio of the 6-month to 0-month lead forecasts (*right column*). Top row is for SST (units oK), *middle row* is for rainfall (units mm/day), and *bottom row* is for 200-mb heights (units

are meters). Standard deviation of ensemble means is a function of the amplitude of the departure from the climatology and is one factor that determines the predictability of seasonal means with regions of larger (smaller) standard deviation related of higher (lower) predictability

EMV of 200-mb height (Fig. 3, bottom row) also has a general decrease with lead-time. One exception is an area of increase in the equatorial Pacific near the dateline that is possibly related to an area of increase in the ensemble mean variance of SSTs (and also in rainfall). Apart from few exceptions, the lead-time dependence in the EMV for all the variables, in general follows what is expected based on conceptual reasoning, i.e., as the lead-time increases, the ensemble mean of predicted SST (for a fixed target period) evolves towards the climatological mean; anomalous SST forcing for the atmosphere decreases, as a consequence the ensemble for atmospheric variables asymptotes towards the climatology, and the EMV decreases.

The conceptual picture also implies that the internal variability of seasonal means for the target season would increase with the lead-time of prediction. This is confirmed in Fig. 4 (top row) where almost everywhere SST internal variability for 6-month predictions is larger than for the 0-month lead predictions. The spatial structure for the evolution of rainfall is more complicated, and again, is because of the dependence of rainfall on the variability of SSTs, as well

as on the mean SST (and on the evolution of SST bias with lead-time). Finally, internal variability for 200-mb heights, similar to that of SSTs, has a general increase with lead-time.

Lead-time dependence of EMV and internal variability determines the evolution of predictability (and prediction skill), and the corresponding signal-to-noise (SN) ratio for two lead-times is shown in Fig. 5. For all the variables analyzed, SN ratio decreases with lead-time. The spatial structure of the SN ratio for rainfall and 200-mb is consistent with prior estimates based on the analysis of AMIP simulations (Trenberth et al. 1998; Peng et al. 2000; Kumar et al. 2007). Specifically: for rainfall, SN ratio for 0-month lead forecast is largest in the tropics and decreases in the extratropical latitudes. In the tropics the SN ratio is highest in the eastern equatorial Pacific and is related to the ENSO variability. For the 200-mb heights, the spatial structure of SN ratio also conforms to the earlier estimates based on the AMIP simulations with largest SN ratio in the tropical latitudes and a general decrease in the extratropical latitudes. For both rainfall and 200-mb height, there are no regions in extratropical latitudes where SN ratio exceeds one.

## STDV OF ENSEMBLE SPREAD (DJF 82–07)

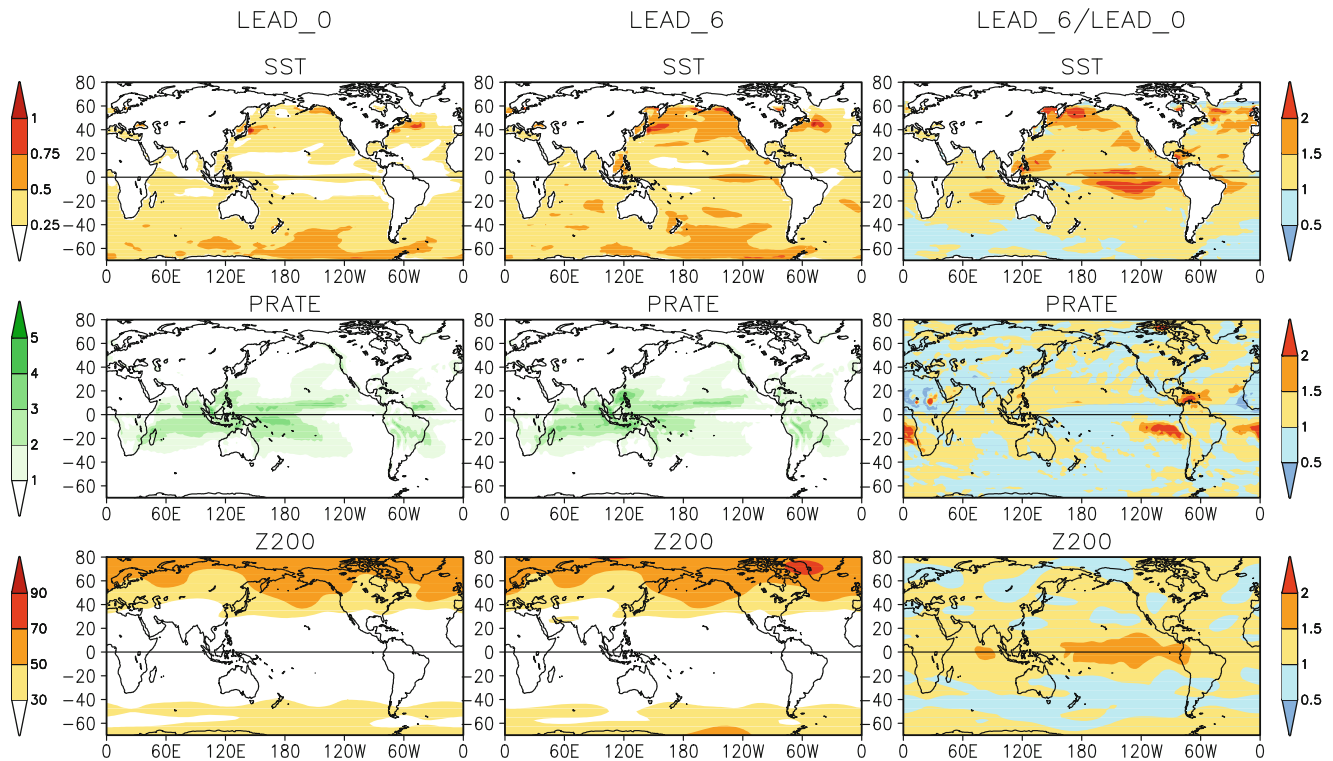


**Fig. 4** Same as for Fig. 5 but for the spread of individual forecasts from the ensemble mean (i.e., the internal variability or the ensemble spread). Predictability of seasonal means is inversely related to the amplitude of the ensemble spread

The SN ratio for SST prediction is unique to the analysis of the coupled model hindcasts (and for which no AMIP counterpart exists). For both lead-times the SN is highest in the eastern equatorial tropical Pacific related to the ENSO. Other region with the high SN ratio is southeast of Greenland. For 0-month lead prediction, SST SN ratios in excess of one are spread over wide geographical regions that includes Indian and Atlantic Ocean, and extratropical oceans in the northern hemisphere. Preference for higher SN in for the northern oceans is likely because of deeper mixed layer during boreal winter (resulting in larger persistence of initial SST anomalies). For longer lead SST prediction in tropics, only regions with SN larger than one are in the Pacific, while SN (and predictability) for the Indian and Atlantic SST is smaller. A point to note is that for 0-month lead, high SN ratio for SST over a wide area does not translate into a similar distribution for the atmospheric variables, possibly indicating that the atmospheric seasonal variability is not constrained by high predictability of local SSTs.

A summary of lead-time dependence of SN ratio is shown in Fig. 6 where area averaged over selected regions EMV and internal variance, and their ratio, is illustrated. All variances are normalized by the EMV for 0-month lead. For the atmospheric variables, features to

note are: only a small further increase in internal variance beyond 0-month lead; a reduction in the EMV with lead-time; reduction in SN ratio with lead time; for 200-mb heights the EMV being larger than the internal variance in the tropics at all lead times, but being dominated by the internal variance in the extratropics. For SST, the EMV stays almost constant for prediction for lead-time up to 3 months, and is due to the high persistence of initial SST anomalies from September onwards. For predictions beyond 3 months there is a gradual decline in the EMV. Although one can extrapolate and estimate the SN (and predictability limits for SST) for longer leads, possible influence of SST prediction going through the spring barrier makes such an assessment a risky conjecture.

An important point to note is that for the shortest lead-time, i.e., 0-month, the internal variance of *atmospheric variables* is already a large fraction of internal variance for longer lead-time predictions indicating that the spread among ensemble members for seasonal means grows quickly. As a consequence atmospheric seasonal predictions (and predictability) may benefit much from the use of atmospheric initial conditions. On the other hand, however, use of correct atmospheric initial conditions may be of importance for coupled SST predictions.

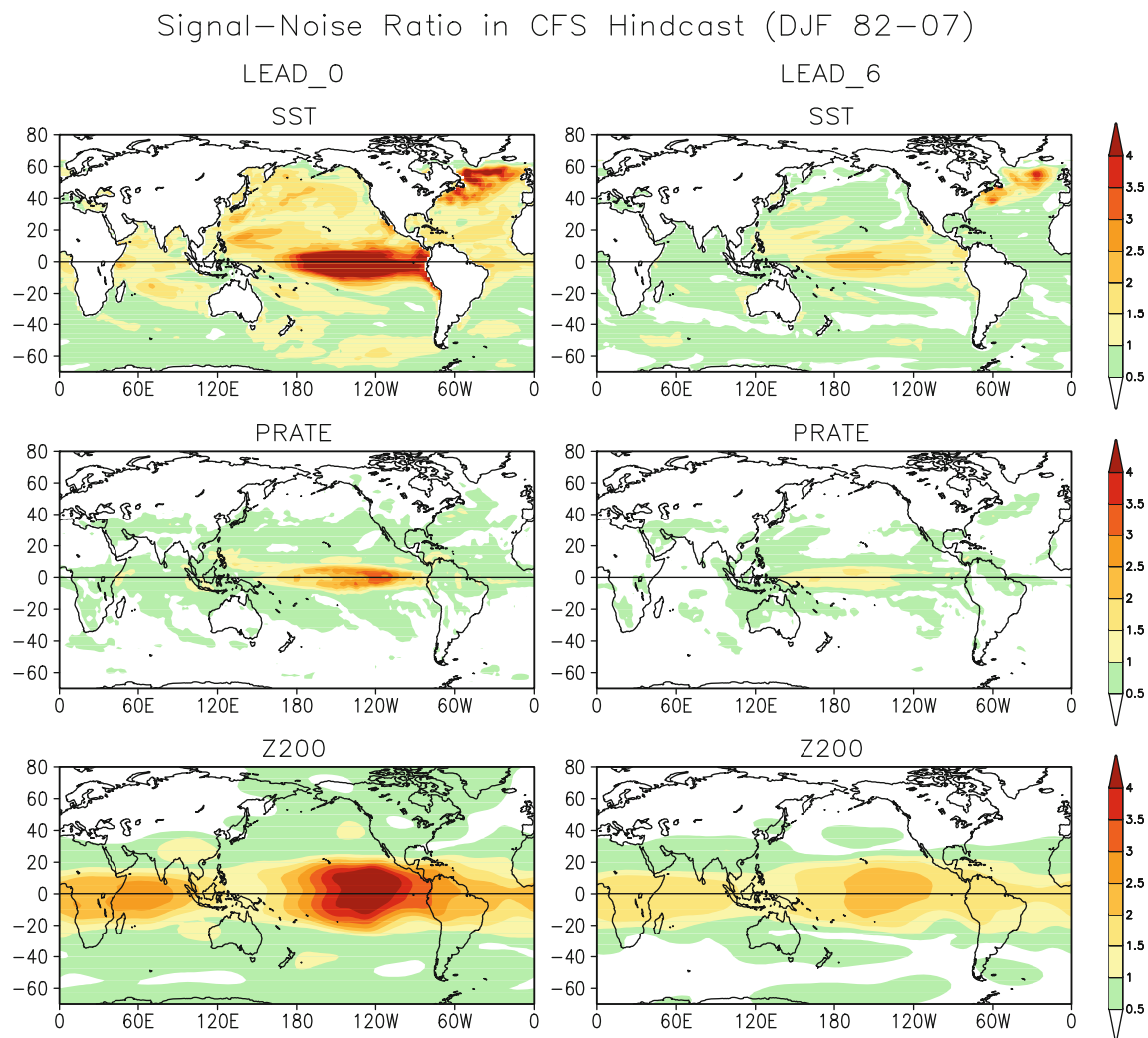


**Fig. 5** Signal-to-Noise (SN) ratio for SSTs (*top row*), rainfall (*middle row*), and 200-mb heights (*bottom row*) for 0-month lead (*left column*), and 6-month lead (*right column*) forecasts. The SN ratio is computed as the ratio of standard deviation of ensemble means

(*Fig. 5*), and standard deviation of individual forecasts from the ensemble mean forecast (*Fig. 6*). Larger (small) SN ratio is indicative of higher (lower) predictability

The SN for precipitation and 200-mb height is next compared with that estimated from the AMIP simulations based on the atmospheric component of the CFS. AMIP estimates are based on an 18-member ensemble for 1996–2009, and although the integration period differs from the CFS, the intent is only to compare the large-scale features.

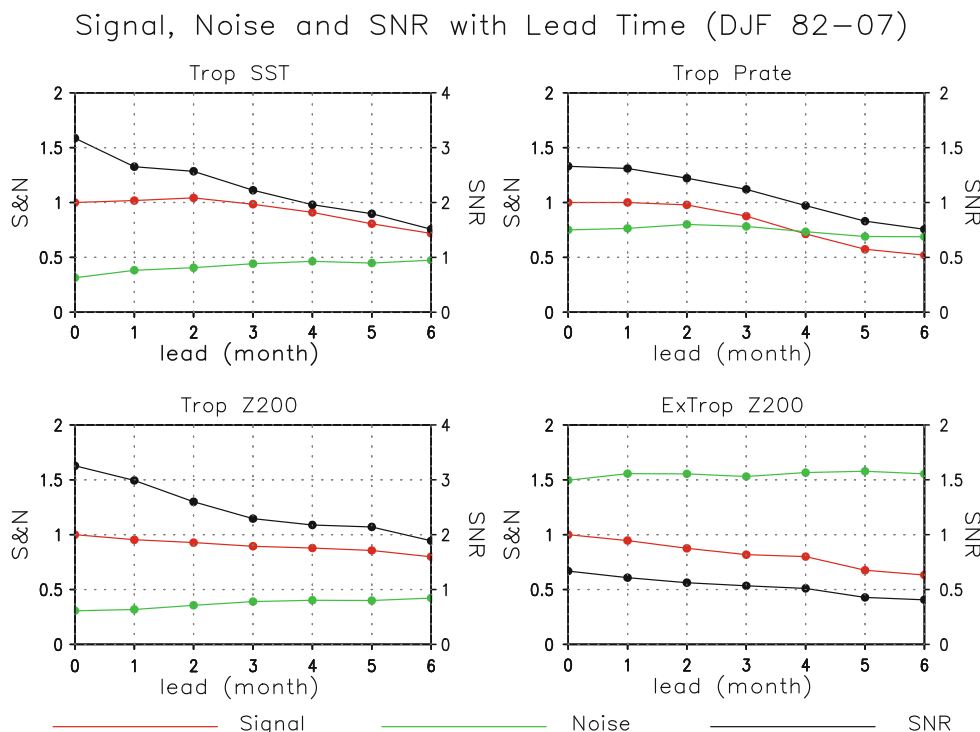
Shown in *Fig. 7* is the SN for precipitation (*top panel*) and 200-mb height (*bottom panel*), and these estimates are compared with that based on the CFS with 0-month lead forecast (*Fig. 5*, *left column*). Broadly, the spatial distribution of SN for the AMIP simulations—higher values in the tropical latitudes, and lower values in the extratropics; higher SN for precipitation in the eastern tropical Pacific—are similar to that for the CFS. This similarity indicates that the lack of initial condition information in the AMIP

simulations, as well as differences in the representation of air–sea interaction, does not result in significantly different estimates for SN and predictability of atmospheric seasonal means.

The similarity in the SN between the CFS and the AMIP is consistent with earlier results. For example, Kumar et al. (2008) analyzed coupled and uncoupled hindcasts and concluded that characteristics of atmospheric seasonal variability were similar. Kumar et al. (2007) and Jha and Kumar (2009) compared SN based on AMIP simulations from multiple AGCMs and reported results similar to presented here based on a single model. Analysis of atmosphere alone AGCM simulations where atmospheric initial conditions are initialized also result in SN similar to those reported here (Shukla et al. 2000; Chang et al. 2000; Phelps et al. 2004).



**Fig. 6** Lead-time dependence of the signal (red curve), noise (green curve), and the signal-to-noise ratio (black curve). The lead-time of the forecast is indicated on the x-axis. Different panels are for the tropical SST (top, right panel), tropical precipitation (top, left panel), tropical 200-mb heights (bottom, left panel), and extratropical 200-mb heights (bottom, right panel). Area averaged signal and noise for tropical fields are area averaged over (180°–270°E; 20°S–20°N) while the extratropical fields are area averaged over (180°–270°E; 30°–80°N) in Figs. 5 and 6



Another question we analyze is: even though the spread of seasonal means increases rapidly, does the ensemble mean atmospheric response has lead-time dependence, or does it also converge to the response to the SST. To analyze the lead-time dependence of the spatial structure of ensemble mean anomalies, we compute the anomaly correlations between the ensemble mean anomalies with different lead times.

The spatial anomaly correlation (AC) for the ensemble mean 200-mb heights over the tropics and northern hemisphere, together with the AC for the ensemble mean predicted SSTs over the tropical Pacific are shown in Fig. 8. The years are arranged according to the absolute value of the observed Niño 3.4 SST index. The anomaly correlations are between ensemble mean predicted anomaly for 0-month and 1-month lead predictions (Fig. 8, top panel), and 0-month and 2-month lead predictions (Fig. 8, bottom panel). The anomaly correlations for the SST anomalies between 0-month and 1-month lead predictions, irrespective to the amplitude of Niño 3.4 SST index, are all generally larger than 0.8. For the AC between 0-month and 2-month lead SST predictions the same also holds true for ENSO events (i.e., when Niño 3.4 SST is large).

As for the atmospheric response of 200-mb heights, anomaly correlations primarily follow the amplitude of Niño 3.4 SST. This indicates that for strong ENSO events, when the atmospheric response is also strong, the spatial structure of the atmospheric anomalies with different lead-time is similar. For weaker SST events, small anomaly correlation

are basically due to weaker atmospheric response, and a larger contribution from the internal variability that a 15-member ensemble mean is not large enough to remove. This conclusion is supported by additional analysis (not shown) that for different lead-time the root mean square (RMS) of the ensemble mean 200-mb anomalies is linearly related with amplitude of the ENSO SSTs.

For the two warm events of DJF 1998 and DJF 2003 the ensemble mean 200-mb heights are shown in Fig. 9, and are also compared with those from the AMIP simulations. The spatial anomaly correlation for 1-month, 2-month lead prediction, and for AMIP simulation with the 0-month lead prediction are also indicated. The spatial structure of 0-month seasonal means is very similar to the longer lead predictions, and is reflected by high spatial correlations. There is also a high degree of spatial resemblance with the AMIP simulations. This implies that the spatial pattern of ensemble mean response for the CFS predictions is largely consistent with the SST anomaly. An additional point to note is that the spatial structure of predicted seasonal mean anomalies is also quite similar for the two warm events, a result also consistent with an earlier analysis by Kumar and Hoerling (1997).

#### 4 Summary

The focus of the analysis was the seasonal predictability for the initialized coupled predictions and an assessment of how the seasonal predictability evolves with the lead-time.

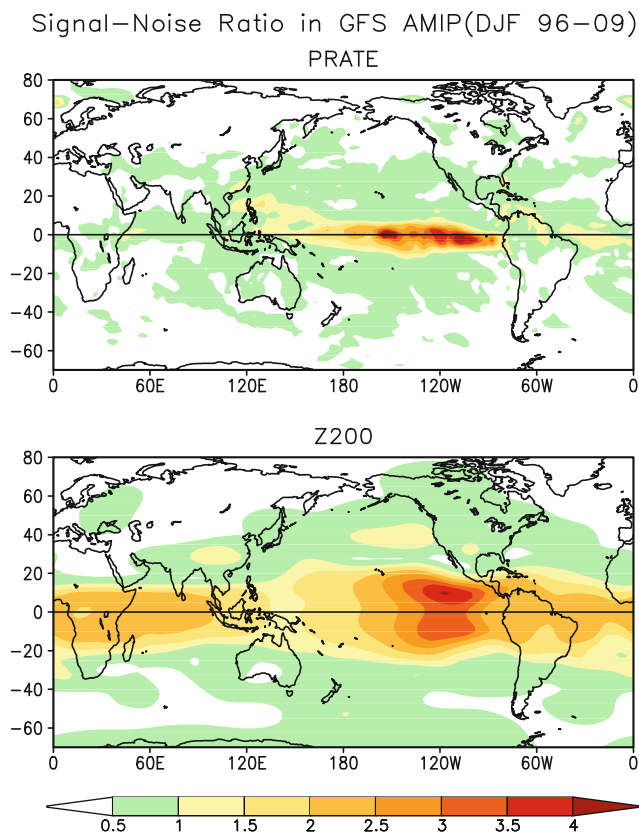


**Fig. 7** Signal-to-Noise (SN) ratio for rainfall (*top panel*), and 200-mb heights (*bottom panel*) based on the AMIP simulations for 1996–2009 period. The SN ratio is computed as the ratio of standard deviation of ensemble means, and standard deviation of individual AMIP simulations from the ensemble mean forecast. Larger (*small*) SN ratio is indicative of higher (*lower*) predictability due to SSTs

For the atmospheric variables, the analysis indicates that starting from clustered initial states the spread of seasonal means among ensemble members evolves quickly. Therefore, an expectation that seasonal means for short lead-time predictions will have smaller spread, and higher predictability, is not realized. Further, the spatial structure of predicted seasonal mean anomalies is also largely consistent with the SST anomalies, and is also similar to the atmospheric response to SSTs inferred from the AMIP simulations. This indicates that in the initialized coupled simulations the atmospheric response of seasonal means quickly becomes consistent with the anomalous SSTs. This result conforms with the fast adjustment time-scale of the atmospheric response to changes in tropical forcing (Jin and Hoskins 1995), and indicates that the predictability of second kind dominates. For SST, and for the DJF as the target season, SN ratio stays high for 6-month long lead forecasts. To obtain a firmer estimate for SST predictability limits, a set of longer lead hindcasts would be required to extrapolate beyond the spring barrier that may constrain the predictability with longer leads.

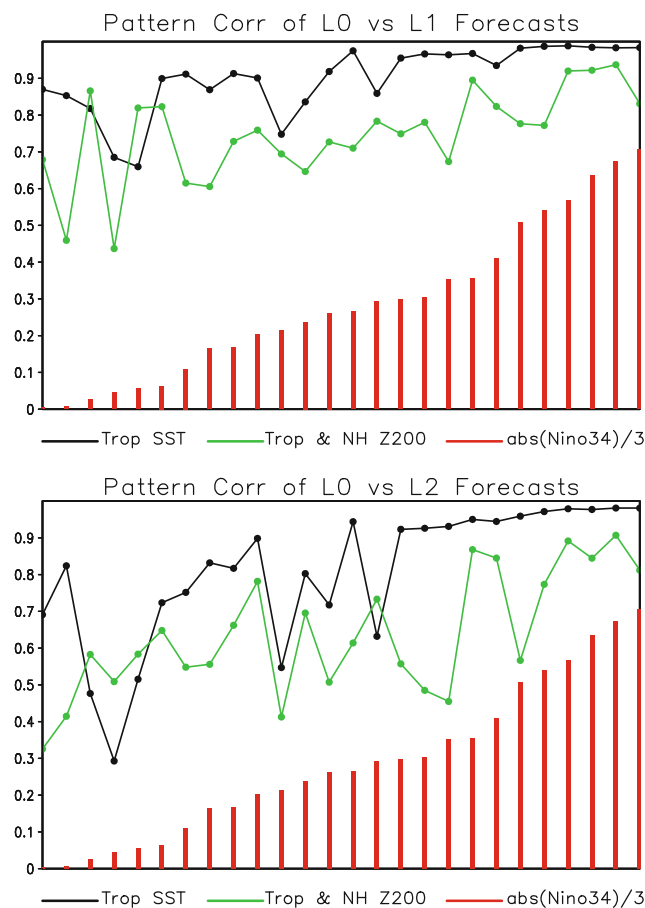
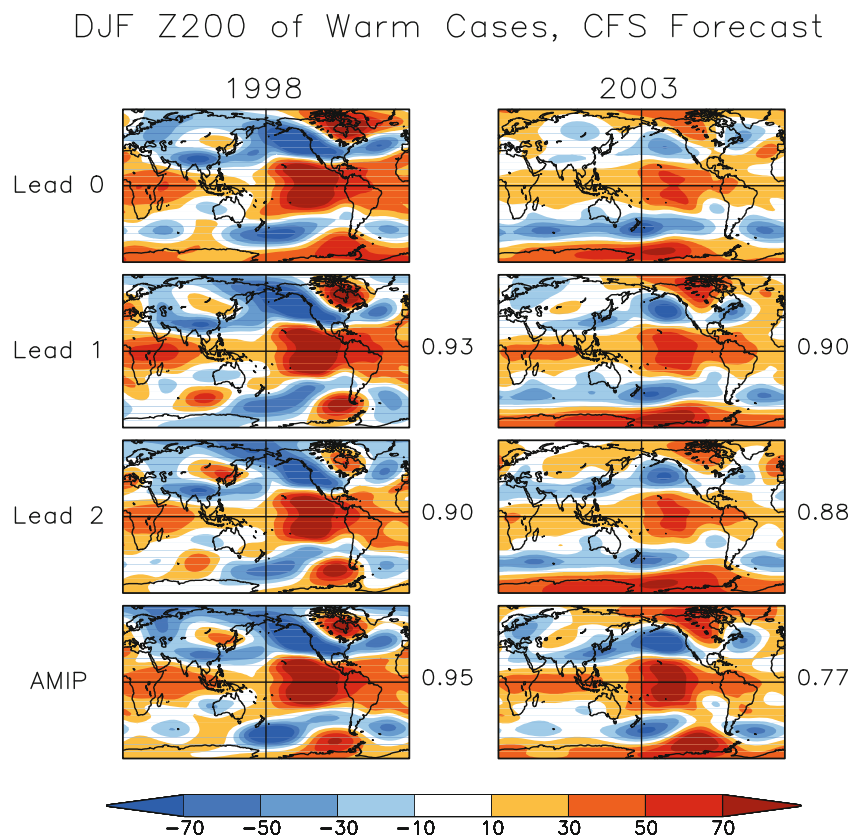


**Fig. 8** Spatial pattern correlation between 0-month and 1-month lead forecast (*top panel*) and between 0-month and 2-month lead forecast (*bottom panel*). The *black curve* is for the SSTs in the tropics (defined as 120°E–280°E, 20°S–20°N) and the *green curve* is for the tropical and northern hemisphere heights (defined as 0–360, 20°S–80°N). The absolute value of the observed Niño 3.4 SST index for the respective years are shown as the vertical bars and years are arranged in the ascending order of amplitude of the Niño 3.4 SST index

Other facts of seasonal predictability of atmospheric means, for example, SN ratio of rainfall and 200-mb heights being largest in the tropical latitudes, and seasonal predictability being low in the extratropical latitudes are consistent with earlier estimates of predictability based on the AMIP simulations. Indeed, the first results assessing the SN for seasonal atmospheric variability based on ensemble of AMIP simulations that appeared around 1995 (for example, Kumar and Hoerling 1995; Harzallah and Sadourny 1995) have withstood the improvements in models, and simulations over a longer period. Therefore, it might now be a definitive conclusion that atmospheric seasonal predictability falls under the paradigm of the predictability of second kind.

Some recent analysis has also documented that the seasonal mean atmospheric variability is not very different between coupled and uncoupled simulations (Kumar et al.

**Fig. 9** The spatial pattern of 200-mb height for 0 month (*row one*), 1 month (*row two*), 2-month (*row three*) for the CFS prediction, and for AMIP simulation (*row four*). The left column is for DJF 1998, and the *right column* is for DJF 2003. The spatial anomaly correlation between the CFS forecast with 0-month lead and forecast with 1-month lead, 2-month lead, and the AMIP simulation is the numerical value listed in between the columns



2008; Jha and Kumar 2008). This result is of considerable relevance for climate attribution studies for the atmospheric variability that rely extensively on the AMIP simulations forced with SSTs. The analysis also has implications for the feasibility of time-slice experiments for the climate projection scenarios, where to generate a larger ensemble, and to provide information on a higher spatial resolution, AGCM simulations are forced with the SST obtained from the coupled climate projection simulations.

The mix of predictability of the first and the second kind in coupled predictions also raises interesting issues for the design of long-range prediction systems, and also for the initialization of slow and fast variables. On the one hand, for the prediction of atmospheric variables, a fast decay time-scale of the information from the initial conditions calls for shortest possible lead-time (as is the case for weather predictions). For the prediction and initialization of slowly evolving variables, ocean for example, it is desirable to have an adequate representation of slowly evolving component. This may call for a sampling of initial ocean states over a longer time period. What is an adequate mix for two opposing influences for the design of long-range prediction strategies remains an open question. Similar issues are likely to become more important for even longer lead initialized predictions, for example, decadal.

An added issue in the sampling of initial conditions is the lead-time dependence in the construction of seasonal forecasts based on lagged ensembles. For the forecast for the first season, it is desirable to construct lagged ensembles from initial conditions closet to the target season (for the persistence of SST is high). For longer lead predictions, sampling over a wider spectrum of ocean initial conditions may be more desirable to increase the reliability by encompassing a broader range of possible outcomes. Once again, what is an adequate strategy remains an open question.

The results also imply that our ability to provide improved seasonal forecast for atmospheric and terrestrial variables with longer and longer lead-time is critically dependent on improving long-lead SST predictions, particularly in the tropical eastern Pacific SST variability related to ENSO. With the emerging focus on the initialized decadal predictions (Meehl et al. 2009), and control SSTs have on the terrestrial climate variability (Hoerling et al. 2008a, b), understanding predictability and prediction of SSTs in other ocean basins would also be an important issue. Further, an analysis similar to the seasonal time-scales could be extended to the decadal prediction of indices of modes of coupled ocean–atmosphere variability, e.g., the Pacific Decadal Oscillation (PDO), the Atlantic Multi-decadal Oscillation (AMO).

**Acknowledgments** Constructive comments by two anonymous reviewers and by Drs. M. Chelliah and Hui Wang greatly improved the final version of the manuscript.

## References

- Barnston AG, Kumar A, Goddard L, Hoerling MP (2005) Improving seasonal predictions practices through attribution of climate variability. *Bull Am Meteor Soc* 85:59–72
- Chang Y, Schubert SD, Suarez M (2000) Boreal winter predictions with the GEOS-2 GCM: the role of boundary forcing and initial conditions. *Q J Roy Meteor Soc* 126:2293–2322
- Chen D, Cane MA, Kaplan A, Zebiak SE, Huang D (2004) Predictability of El Niño over 148 years. *Nature* 428:733–736
- Chen M, Wang W, Kumar A (2009) Prediction of monthly mean temperature: the roles of atmospheric and land initial condition and sea surface temperature. *J Clim*, to appear
- Gadgil S, Joseph PV, Joshi NV (1984) Ocean–atmosphere coupling over monsoon regions. *Nature* 312:141–143
- Harzallah A, Sadoury R (1995) Internal versus SST-forced variability as simulated by an atmospheric general circulation model. *J Clim* 8:474–495
- Hoerling MP, Kumar A (2002) Atmospheric response patterns associated with tropical forcing. *J Clim* 15:2184–2203
- Hoerling MP, Kumar A, Eischeid J, Jha B (2008a) What is causing the variability in Global Land Temperature? *Geophys Res Lett* 35:L23712. doi:10.1029/2008GL035984
- Hoerling M, Hegerl G, Karoly D, Kumar A, Rind D (2008b) Attribution of the causes of climate variations and trends over North America during the modern reanalysis period. In: Dole R, Hoerling M, Schubert S (eds) *Reanalysis of historical climate data for key atmospheric features: implications for attribution of causes of observed change. A report by the U.S. Climate Change Science Program and the Subcommittee on Global Change Research*. National Oceanic and Atmospheric Administration, National Climatic Data Center, Asheville, NC, pp 47–92
- Jha B, Kumar A (2008) A comparison of the atmospheric response to ENSO in coupled and uncoupled model simulations. *Mon Wea Rev* 137:479–487
- Jha B, Kumar A (2009) A comparative analysis of change in the first and second moment of the PDF of seasonal mean 200-mb heights with ENSO SSTs. *J Clim* 22:1412–1423
- Jin F-F, Hoskins BJ (1995) The direct response to tropical heating in a baroclinic atmosphere. *J Atmos Sci* 52:307–319
- Jin E et al (2008) Current status of ENSO prediction skill in coupled ocean–atmosphere models. *Clim Dyn* 31:647–664. doi:10.1007/s00382-008-0397-3
- Kanamitsu M, Ebisuzaki W, Woollen J, Yang S-K, Hnilo J, Fiorino M, Potter GL (2002) NCEP–DOE AMIP-II Reanalysis (R-2). *Bull Am Meteor Soc* 83:1631–1643
- Kug J-S, Kang I-S, Choi D-H (2008) Seasonal climate predictability with tier-one and tier-two prediction systems. *Clim Dyn* 31:403–416
- Kumar A, Hoerling MP (1995) Prospects and limitations of seasonal atmospheric GCM predictions. *Bull Am Meteor Soc* 76:335–345
- Kumar A, Hoerling MP (1997) Interpretation and Implications of the observed inter-El Niño variability. *J Clim* 10:83–91
- Kumar A, Schubert SD, Suarez MS (2003) Variability and predictability of 200-mb seasonal mean heights during summer and winter. *J Geophys Res* 108:4169. doi:10.1029/2002JD002728
- Kumar A, Jha B, Zhang Q, Bounoua L (2007) A new methodology for estimating the unpredictable component of seasonal atmospheric variability. *J Clim* 20:3888–3901
- Kumar A, Zhang Q, Schemm J-KE, L’Heureux ML, Seo K-H (2008) An assessment of errors in the simulation of atmospheric interannual variability in uncoupled AGCM simulations. *J Clim* 21:2204–2217
- Kusunoki S, Sugi M, Kitoh A, Kobayashi C, Takano K (2001) Atmospheric seasonal predictability experiments by the JMA AGCM. *J Meteor Soc Jpn* 79:1183–1206
- Lorenz EN (1969) The predictability of a flow which possesses many scales of motion. *Tellus* 21:289–307
- Luo J-J, Masson S, Behera S, Shingu S, Yamagata T (2005) Seasonal climate predictability in a coupled OAGCM using a different approach for ensemble forecasts. *J Clim* 18:4474–4497
- Luo J-J, Masson S, Behera S, Yamagata T (2008) Extended ENSO predictions using a fully coupled ocean–atmosphere model. *J Clim* 21:84–93
- Meehl GA et al (2009) Decadal prediction: can it be skillful. *Bull Am Meteor Soc* 90:1467–1485
- Newman M, Sardeshmukh PD (1998) The impact of the annual cycle on the North Pacific/North American response to remote low-frequency forcing. *J Atmos Sci* 55:1336–1353
- Palmer TN et al (2004) Development of a European multi-model ensemble system for seasonal to interannual prediction (DEMETER). *Bull Am Meteor Soc* 85:853–872
- Peng P, Kumar A, Barnston AG, Goddard L (2000) Simulation skills of the SST-forced global climate variability of the NCEP–MRF9 and the Scripps–MPI ECHAM3 models. *J Clim* 13:3657–3679
- Phelps MW, Kumar A, O’Brien JJ (2004) Potential predictability in the NCEP/CPC dynamical seasonal forecast system. *J Clim* 17:3775–3785
- Reynolds RW, Rayner NA, Smith TM, Stokes DC, Wang W (2002) An improved in situ and satellite SST analysis for climate. *J Clim* 15:1609–1625
- Rowell DP (1998) Assessing potential seasonal predictability with an ensemble of multidecadal GCM simulations. *J Clim* 11:109–120
- Saha S et al (2006) The NCEP climate forecast system. *J Clim* 19:3483–3517
- Shukla J et al (2000) Dynamical seasonal prediction. *Bull Am Meteor Soc* 81:2593–2606
- Tang Y, Debg Z, Zhou Z, Cheng Y, Chen D (2008) Interdecadal variation of ENSO predictability in multiple models. *J Clim* 21:4811–4833
- Trenberth EK, Branstrator GW, Karoly D, Kumar A, Lau N-C, Ropelewski C (1998) Progress during TOGA in understanding and modeling global teleconnections associated with tropical sea surface temperatures. *J Geophys Res* 103(C7):14291–14324
- van den Dool HM, Peng P, Johansson A, Chelliah M, Shabbar A, Saha S (2006) Seasonal-to-decadal predictability and prediction of North American climate—the Atlantic influence. *J Clim* 19:6005–6024
- Wang W, Saha S, Pan H-L, Nadiga S, White G (2005) Simulation of ENSO in the new NCEP Coupled Forecast System Model (CFS03). *Mon Wea Rev* 133:1574–1593
- Wang B et al (2008) How accurately do coupled models predict the leading modes of Asian–Australian monsoon interannual variability? *Clim Dyn* 30:605–619
- Weigel AP, Baggenstos D, Liniger M, Vitart F, Appenzeller C (2008) Probabilistic verification of monthly temperature forecasts. *Mon Wea Rev* 136:5152–5182
- Xie P, Arkin PA (1997) Global precipitation: a 17-year monthly analysis based on gauge observations, satellite estimates, and numerical model outputs. *Bull Am Meteor Soc* 78:2539–2558
- Zwiers FW, Wang XL, Sheng J (2000) Effects of specifying boundary conditions in an ensemble of atmospheric GCM simulations. *J Geophys Res* 105:7295–7315